

Analysis of the Possibility of Forming Stiffening Ribs in Litecor Metal-Plastic Composite Using the Single Point Incremental Forming Method

KUBIT Andrzej^{1,a*}, KORZENIOWSKI Marcin^{2,b}, BOBUSIA Michał^{3,c},
OCHAŁEK Krzysztof^{3,d} and SLOTA Ján^{4,e}

¹Department of Manufacturing and Production Engineering, Rzeszow University of Technology, al. Powst. Warszawy 8, 35-959 Rzeszów, Poland

²Department of Metal Forming, Welding and Metrology, Faculty of Mechanical Engineering, Wrocław University of Science and Technology, Wyb. Wyspiańskiego 27, 50-370 Wrocław, Poland

³Department of Mechanics and Machine Building, Carpatian State School in Krosno, ul. Żwirki i Wigury 9A, 38-400 Krosno, Poland

⁴Institute of Technology and Materials Engineering, Faculty of Mechanical Engineering, Technical University of Košice, Mäsiarska 74, 040 01 Košice, Slovakia;

^{a*}akubit@prz.edu.pl, ^bmarcin.korzeniowski@pwr.edu.pl, ^cmichal.bobusia@kpu.krosno.pl,
^dkrzysztof.ochalek@kpu.krosno.pl, ^ejan.slota@tuke.sk

Keywords: Litecor sandwich structure, metal-plastic composites, stiffening rib; incremental sheet forming; SPIF.

Abstract. Efforts to reduce CO_x are extremely important, which forces the use of materials and technologies that reduce the weight of means of transport in order to reduce energy consumption. Currently, aluminum alloys and FRP composites are still too expensive for mass industry applications. Presented in this study, Litecor is a three-layer composite that combines the high strength of steel with the low density of plastic. Thanks to the use of external steel covers 0.3 mm thick and a light core 0.7 mm thick, high stiffness was achieved while maintaining a relatively low weight. The weight reduction in comparison with steel blanks with the same stiffness is up to 40%. Litecor is mainly developed by ThyssenKrupp, it is a promising construction material, but it requires development the technology of forming and joining.

In this study, the possibility of forming the Litecor layered composite was investigated using the single-point incremental sheet forming (SPIF) method. As part of the research, the stiffening ribs were shaped, the maximum depth of the embossing was determined. The degree of thinning in selected cross-sections of the embossing was determined. The influence of the rotational speed of the tool and the feed rate on the properties of the shaped surface was also analyzed. Incorrectly selected shaping parameters have been shown to damage the zinc coating on the inner surface of the embossing.

Introduction

Incremental sheet forming (ISF) is a relatively new plastic forming technology, characterized by flexibility, low tooling costs, and may be an alternative to traditional stamping processes in the case of unit production, small series, and also in prototyping processes [1-3]. While reviewing the research carried out on this subject, it can be observed that ISF technology is increasingly used to form lightweight structures in the aviation, maritime, and automotive industries [4, 5]. An important feature of ISF technology, which is flexibility, made the discussed forming method to be used in medicine, among others for the manufacturing of highly customized medical products [6]. It is a suitable method for the production of parts of prostheses and orthoses [7].

Although the most commonly discussed forming technology is used for the shaping of metal sheets [8, 9], ISF can also be successfully used for other materials [10, 11]. The authors of the work [12] present the effectiveness of shaping complex spatial shapes in conditions of elevated temperature

of thermoplastic polymers, such as polytene, polyamide, polyvinyl chloride, polycarbonate. In turn, work [13] presents research on shaping glass fiber reinforced polyamide, which is a material widely used in automotive applications.

The effectiveness of ISF shaping in relation to individual materials is determined by the correct selection of process parameters. The basic parameters are: tool rotational speed, feed, stroke, tool geometry, and lubrication conditions. There are many studies available in which the authors described the influence of particular parameters on the properties of shaped elements [14-18]. The use of lubrication with different properties, as well as the rotational speed of the tool, has the greatest impact on the friction conditions and thus the force values of the tool on the shaped material [19- 23]. Bagudanch et al. [24] showed that tool diameter and step size have a significant impact on the resistance forces in the shaping process.

Due to global trends in reducing CO_x, an increasing tendency is observed to reduce the mass, especially of means of transport [25-27]. Therefore, more and more often composite materials are used to enable the production of structures with high strength and stiffness while maintaining a relatively low weight [27]. Polymer-fiber composites (FRP) are currently still too expensive in terms of technology to be widely used in the mass industry. Metal-plastic composites (MPCs) are one of the promising groups of composites. A representative of this group of materials is the Litecor sandwich composite produced by Thyssenkrupp. It is a lightweight, three-layer composite made of a polymer core and two outer covers of galvanized steel.

Litecor materials are characterized by a relatively high resistance to bending compared to aluminum or steel. With a total thickness of 1.3 mm, the composite is more stiff than a sheet made of an aluminum alloy [28].

Currently, Litecor has been used to produce body parts of high-performance cars (e.g. Volkswagen Polo R WRC). In the near future, Litecor is planned to be used on car body parts to reduce weight. To be able to use a new type of composite materials composed of various phases more widely, it is necessary to develop effective methods of joining and plastic forming. Currently used methods for joining Litecor composites are, among others, mechanical fastening (e.g., self-piercing riveting, clinching), joining by forming (e.g., hemming, seaming), resistance spot welding, and adhesive bonding [29-33]. On the other hand, traditional stamping methods are used for plastic shaping. The more and more widely used flexible ISF technology that does not require expensive tooling can also be effective in the cold forming of Litecor composites.

This work aims at the implementation of experimental research that determines the possibilities of shaping Litecor layered composites using the single-point incremental forming (SPIF) method. Research was carried out by forming longitudinal stiffening ribs. The paper presents a preliminary selection of forming parameters and lubrication conditions. The quality of the shaped surface was assessed.

Materials and Methods

As part of the research, material from the MPCs group, Litecor, was formed. It is a lightweight, three-layer composite made of a polymer core and two outer layers of galvanized, interstitial atom-free steel. The core consists of 52% polyamide PA6, 36% polyethylene, and additives. The covers are made of CR210IF steel (Thyssenkrupp), it is cold-rolled steel. In order to protect against corrosion, covers with a protective zinc layer are used. Litecor comes in two variants: Litecor C (classical, used in this research) and Litecor S (strong) [34].

In the presented research, a 1.3 mm thick composite was used, the cover thickness of which is 0.3 mm, and the polymer core is 0.7 mm. Table 1 presents the basic mechanical properties provided by the manufacturer [34].

Table 1. Mechanical properties of Litecor C [34].

Thickness, t mm	Yield Strength, R _{0.2} MPa	Ultimate Tensile Strength, R _m MPa	Total Elongation, A ₈₀ %
1.3	120-180	190-240	28

As a forming tool was used HS2-9-2 (1.3348) steel pin with a rounded tip with a radius of $r = 2.5$ mm. In order to reduce the coefficient of friction during the forming process, lubrication was applied using Mannol FWD Getriebeöl SAE 75W-85 gear oil (Mannol, Wedel, Germany). The basic properties of the oil used were provided by the manufacturer and are as follows: density 879 kg/m^3 (at 15°C), flash point 210°C , pour point -45°C , viscosity at 40°C $72.4 \text{ mm}^2/\text{s}$, viscosity index 157. The device (Figure 1) for incremental forming was mounted in the table of a numerically controlled TM-1P vertical milling machine (Hass Automation, Oxnard, CA, USA).

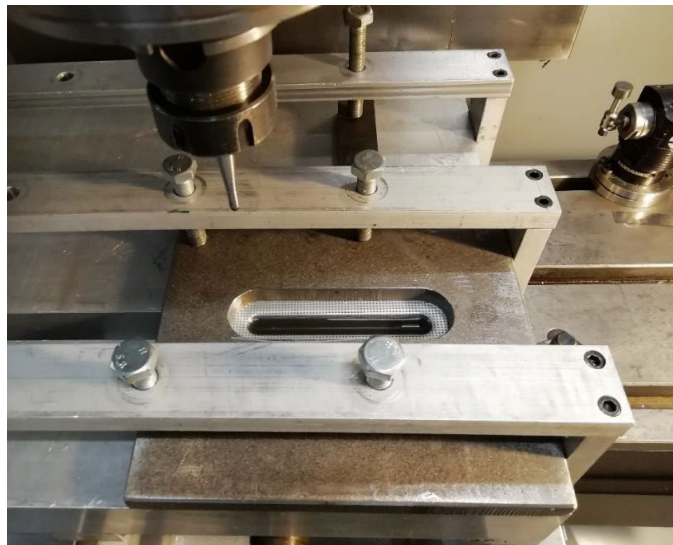


Fig. 1. Device for incremental forming mounted in the table of a numerically controlled Haas TM-1P vertical milling machine.

The strain distribution of the sheet material in the area of the ribs was determined using the Argus (GOM Gmbh, Braunschweig, Germany) non-contact material-independent measuring system based on digital image correlation. The measurement was carried out by referring to the change in the position of black points, with a diameter of 1 mm, which were etched onto the surface of the panel before the SPIF process. The sample on the test stand equipped with a 12-megapixel camera sensor is shown in the Fig. 2.

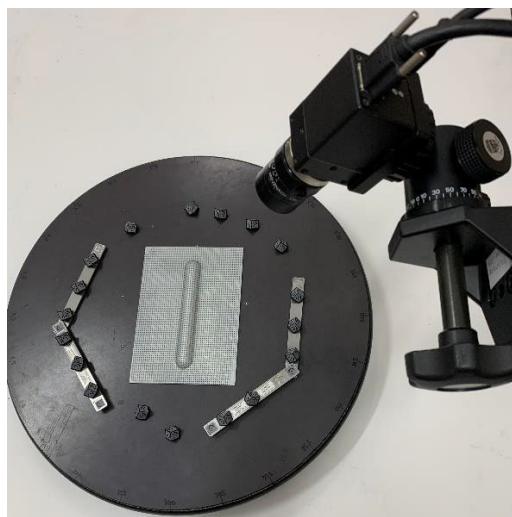


Fig. 2. The GOM-Argus measurement setup.

The embossing was formed in Litecor C composite panels with dimensions of 100x160 mm (Fig. 3). The formed stiffening ribs were 120 mm long and 20 mm wide. The embossing depth D was selected experimentally. A simple tool with a longitudinal groove with the target crease width was used as a forming matrix. The shaping was performed first with the use of basic parameters selected on the basis of the authors' previous experiences [35, 36]. The forming process was carried out using a continuous spiral-shaped toolpath. The vertical pitch value of $a_p = 0.4$ mm was assumed, the spindle rotation speed $n = 300$ rpm and the feed rate $f = 1500$ mm/min were established. To prepare the control program, the Edge CAM program (Hexagon AB, Stockholm, Sweden) was used. The morphologies of the shaped surfaces of the panels and the analysis of the chemical composition by the EDS method were examined using an S-3400 scanning electron microscope (SEM) Phenom ProX (Nanoscience Instruments, Phoenix, AZ, USA).

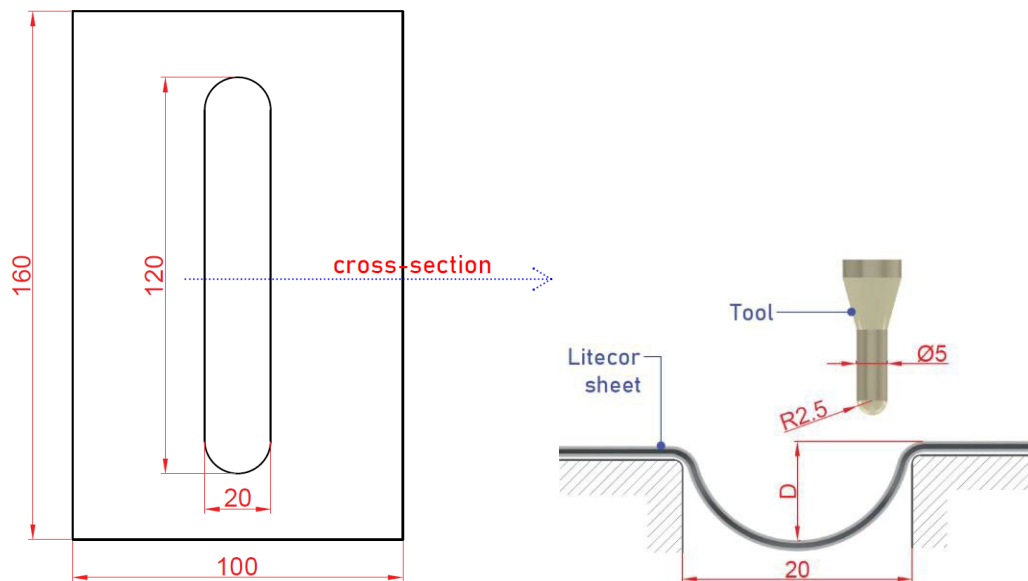


Fig. 3. Dimensions (in mm) of a rib-stiffened panel and the tool using in the experiments.

Results and Discussion

Using the basic parameters, first the maximum depth of the stiffening rib was determined by an experimental method. Based on the previous experiences of the authors [35, 36], an attempt was made to form an embossing with a depth of $D = 7$ mm. In the forming process, cracking of the outer cover was observed with the tool recess equal to 6.65 mm. The fracture effect is shown in Fig. 4, the fracture was each time initiated on the corner of rib. The crack, along with the additional movement of the tool, propagated along the circumference of the embossment. The cracking occurred in the area of the greatest thinning of the outer cover, at the height of $2/3$ of the embossing depth (Fig. 4b). It was observed that the cracking process was preceded each time by the appearance of the orange peel phenomenon on the outer cover of the composite, which was also illustrated in Fig. 4a.

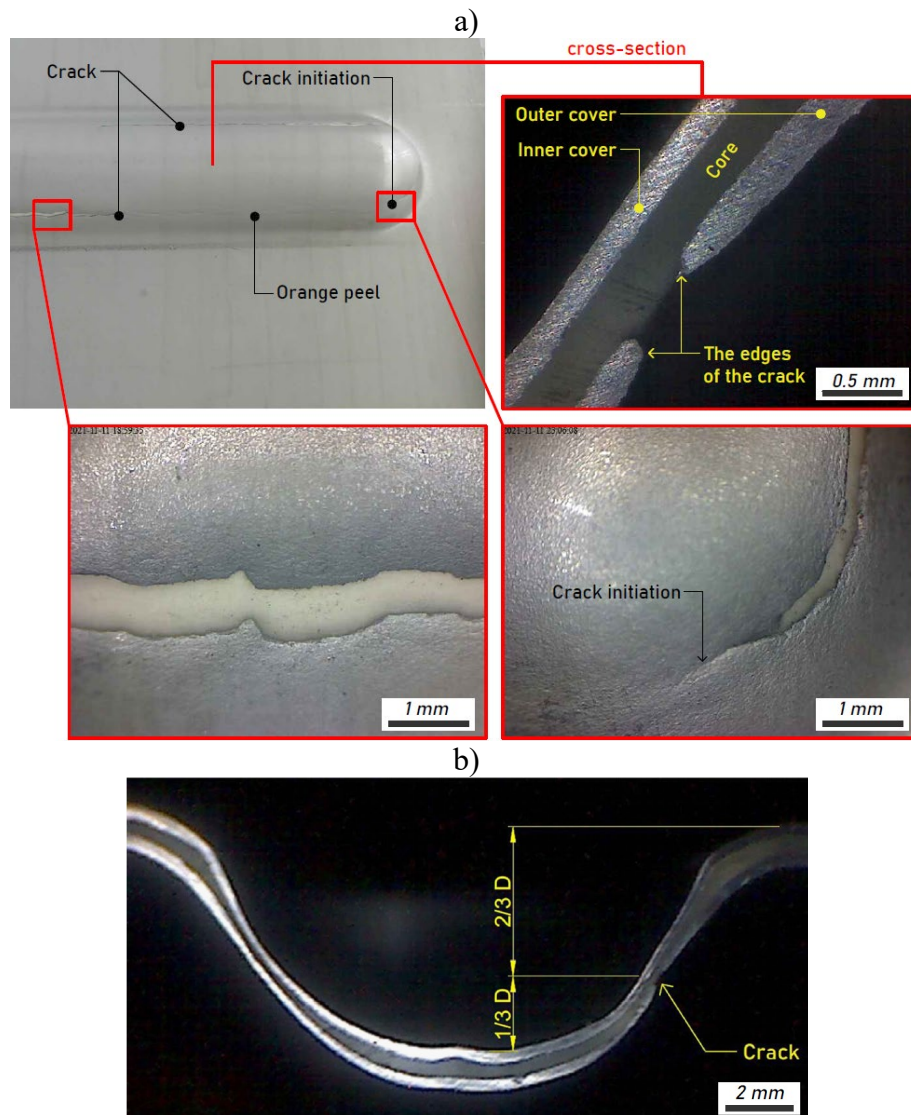


Fig. 4. View of the crack in the outer cover of the Litecor composite for the embossing variant with the depth of the embossing $D = 7$ mm (a) and an indication of the depth at which the crack occurred (b).

In the next step, the embossing geometry was modified by reducing the maximum depth by 0.5 mm in relation to the depth at which the crack initiation was observed in the previous step. Therefore, the formation was carried out for the maximum penetration of the tool with the value of $D = 6.15$ mm. Using the previously adopted basic shaping parameters, the embossments were made according to the assumed geometry and in this case the material did not crack. On the other hand, it was observed that there was a significant strain on the material, as the orange peel phenomenon was shown along the perimeter of the embossing, as shown in Fig. 5. Thus, a slight increase in depth would lead to the appearance of cracks.

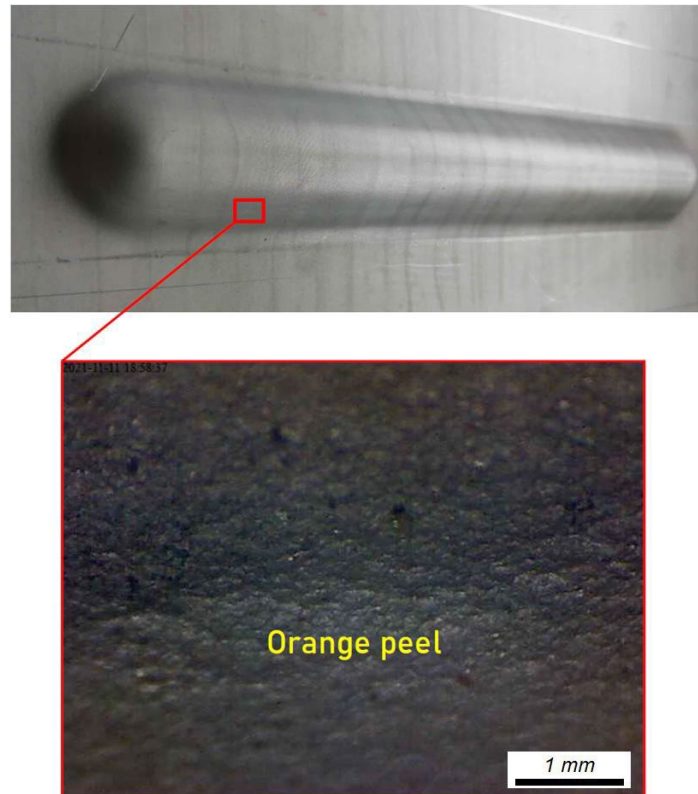


Fig. 5. View of the outer surface of the drawpiece for the variant with the depth of the embossing $D = 6.15$ mm showing the appearance of the orange peel phenomenon.

In the next stage, the maximum depth of the tool was lowered by another 0.5 mm. Therefore, the extrusion geometry was prepared and the CAM program was generated for an extrusion with a depth of 5.65 mm. At this depth, no cracking was observed and no orange peel was observed on the outer lining. The cross-sections of the embossing in various areas and directions were analyzed. Fig. 6a shows a sample with an embossing along with the designation of the planes in which the cross-sections were made. The first of the considered cross-sections is the cross-section to be creased halfway along its length (Fig. 6c). There was a thinning of the shaped material from the original value of 1.3 mm, to the value of 0.75 mm, which is a reduction in thickness by 42.3%. Moving on to the thinning analysis of individual layers, the polymer core layer was reduced by 48% in this cross-section, from the original thickness of 0.7 mm to a thickness of 0.36 mm. In the case of claddings, a thickness reduction of 33.3% (to 0.2 mm) was demonstrated for the internal cladding and 36.7% (to a value of 0.19 mm) for the external cladding.

Going to the cross-section at the end of the embossing, directly in front of the radius (Fig. 6d), a significantly greater reduction in the thickness of the shaped material was shown, namely by 56.2%, the wall was thinned in this cross-section from the original thickness of 1.3 mm to 0.57 mm. The thickness of the polymer core was reduced here by 62.9%, to a value of 0.26 mm. In turn, the cladding was reduced by 50% and by 46.7% for the internal and external cladding, respectively.

The last of the analyzed cross-sections is the cross-section along the embossing, showing its end part (Fig. 6b). The thickness of the composite was thinned to 0.71 mm, which in relation to the original thickness of 1.3 mm indicates a reduction of 45.4%. The core thickness in the section under consideration was reduced by 62.9%. The thickness of the inner cladding was reduced to 0.22 mm, by 26.7%, and the outer cladding thickness to 0.23 mm, i.e. by 23.3%.

As it results from the presented analysis of the reduction of the thickness of individual layers in the cross-sections under consideration, the greatest material stress occurs at the ends of the embossing, hence the crack initiation in the case of too large embossing depth in this area.

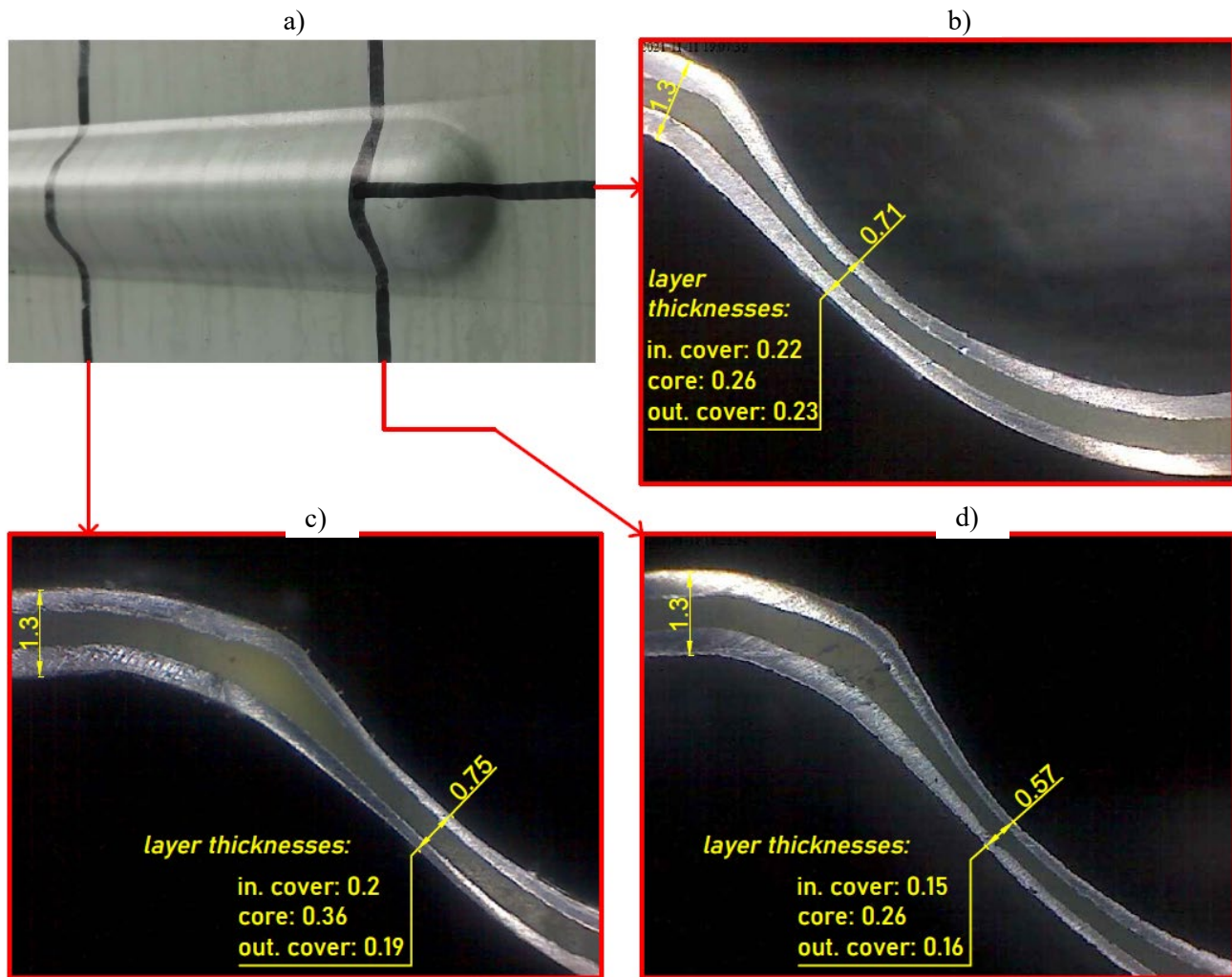


Fig. 6. Cross-sections in characteristic planes showing the thinning of individual composite layers for the variant with the embossing depth $D = 5.65$ mm: (a) general view with marked cross-sections; (b) longitudinal cross-section in the corner; (c) perpendicular cross-section in the middle of the embossment; (d) perpendicular cross-section in the corner.

Measurements of the thinning (Fig. 7) realized by the GOM-Argus method confirmed that the most stress-affected area in the panels is the corner of the rib. Although due to the layered structure of the composite, the measurement carried out is not a precise measurement of individual layers, but the total thinning of the material exceeded 50% at the rib corner was confirmed. However, it should be noted that due to the very slender nature of the rib, the corner of the rib does not play an important role in the compression strength of the panels. It is assumed that this type of stiffening ribs is subjected to compressive stresses in real structures.

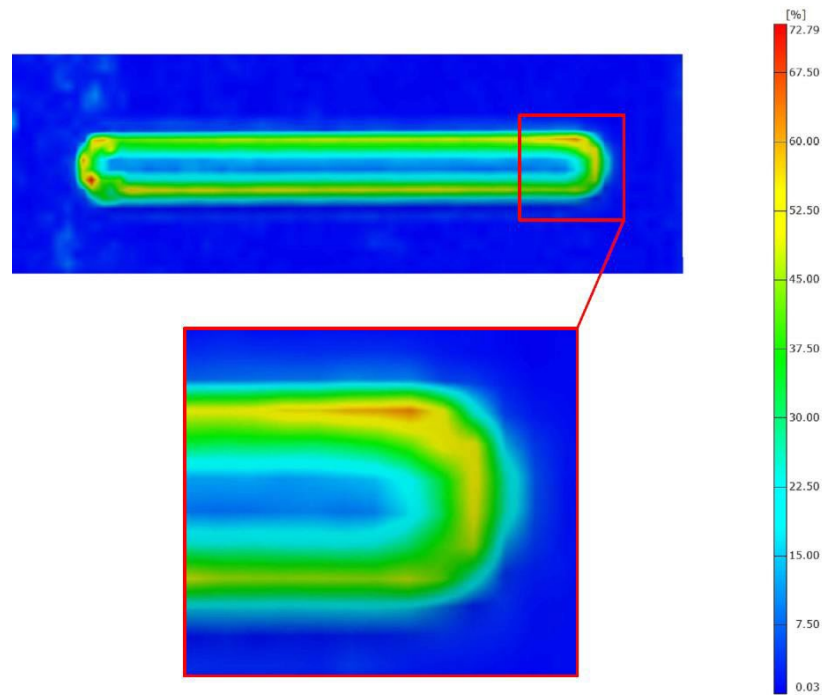


Fig. 7. Distributions of thinning of the rib fabricated in 1.3 mm-thick Litecor C.

After the analysis of different stiffening ribbing depths and indicating the value at which it is possible to obtain the correct embossing, various parameters of the forming process were analyzed in the next stage of the research.

The influence of the increased rotational speed and the increased value of the feed rate on the properties of the inner surface of the embossing was determined. According to the authors of the work [37, 38], the higher the rotational speed, the greater the amount of heat generated due to friction. Therefore, this should lead to the plasticization of the material and thus a reduction of the shaping forces. In order to verify this thesis, the shaping of the stiffening ribs was realized at a rotational speed 10 times higher than in the basic variant. Therefore, the process was carried out at a rotational speed equal to $n = 3000$ rpm, this variant was called 'High rotational speed'.

Of course, the feed rate has an influence on technological time, so it makes sense from an economic point of view to use the highest possible feed rate. Therefore, the influence of twice the value of the feed rate on the surface properties was analyzed. A two-fold increase was assumed, so the feed value $f = 3000$ mm/min was used; this variant was called the „high feed rate“. In addition, the analysis also included a tenfold lower value of the feed in relation to the basic parameters, i.e. $f = 150$ mm / min. On the basis of the analysis of the geometrical properties of the surface, it was found that the reduced value of the feed rate did not have a significant effect on these properties and the low value of the feed resulted in a significant increase in the shaping time. Therefore, this variant was not considered in further analyzes.

Fig. 8a shows views of the internal surfaces of the ribs produced using the parameters described above.

When analyzing the surface shaped using the basic parameters (Fig. 8b), one can observe linear traces in line with the path of the shaping tool.

Both for high feed rate forming (Fig. 8c) and for high rotational speed forming (Fig. 8d), the fractal nature of the surface was observed. As a result of the kinematics of the tool movement, with certain parameters, regular structures of the surface geometry were formed, which is the result of the plastic shaping of the surface of the material, which in this case is zinc, because the covers are galvanized. The phenomenon of breaking and overlapping of the zinc coating layer fragments took place here.

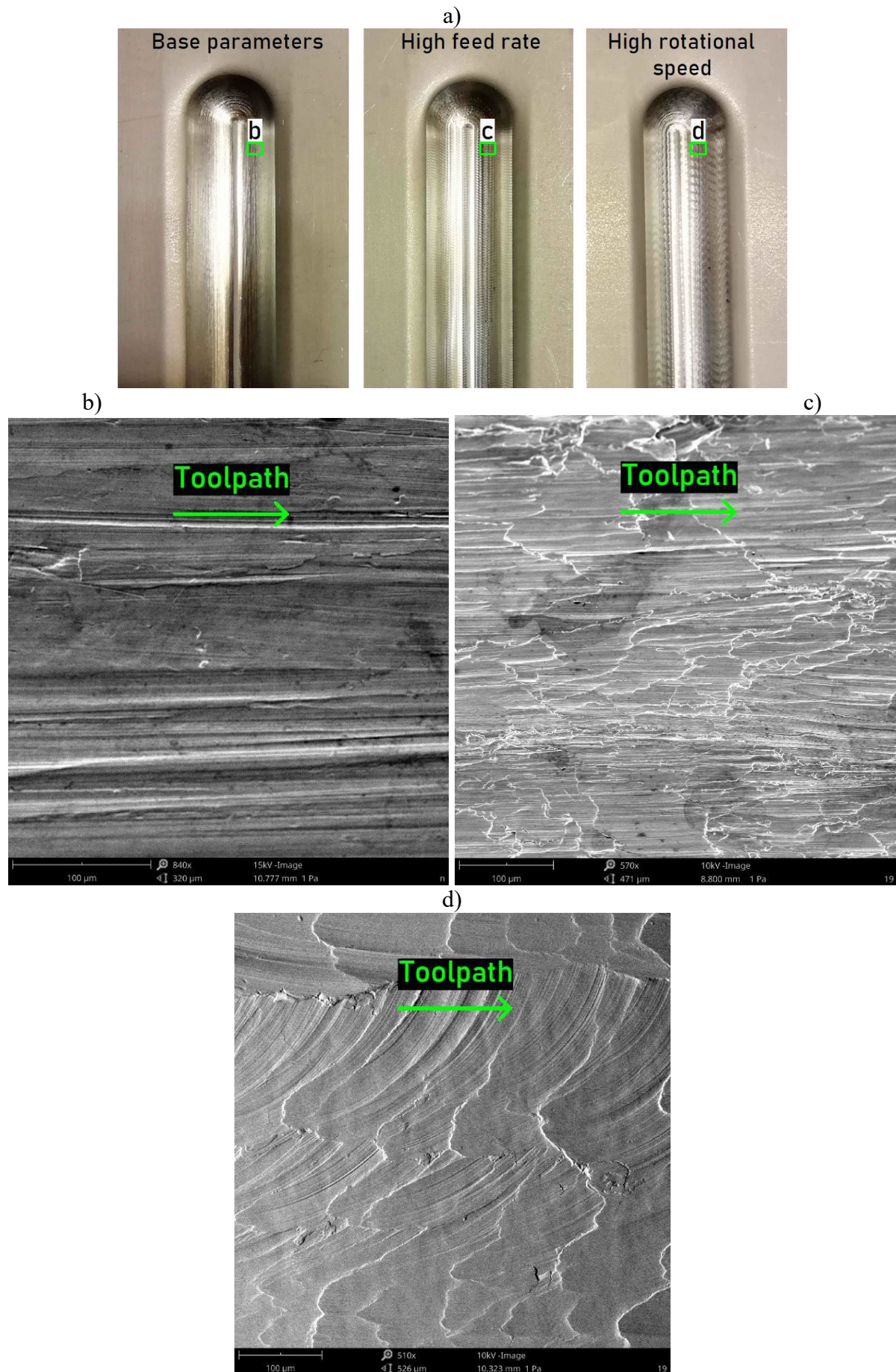


Fig. 8. Macroscopic views of the inner surfaces of the drawpieces (a) and SEM images of these surfaces for the variants: Base parameters (b), High feed rate (c) and High rotational speed (d).

For individual variants, the chemical composition was also analyzed at selected points of the inner surface of the embossments. The analysis was performed using the EDS method, Fig. 9 shows selected points on the surfaces where the chemical composition was determined. These tests were aimed at determining whether the protective zinc coating was damaged in individual variants. Table 2 presents the percentage of elements whose share was shown on the surface at selected points. The test results show that, in the case of the variant produced with the use of basic parameters, the zinc coating was not damaged, which is a positive feature of this case. On the other hand, in the case of the variant made with an increased feed value, the presence of iron on the surface was demonstrated, which proves that the continuity of the zinc coating was broken. A much higher proportion of iron was detected on the surface of the sample produced at a high rotational speed of the tool, 48 wt.%, iron, which proves the phenomenon of zinc coating scuffing, which took place as a result of the parameters of the friction process that occurred at an increased rotational speed of the tool.

The above analysis proves that the originally adopted parameters of shaping the layered composites in question are correct, while increasing the feed value and rotational speed to the indicated values leads to undesirable surface phenomena.

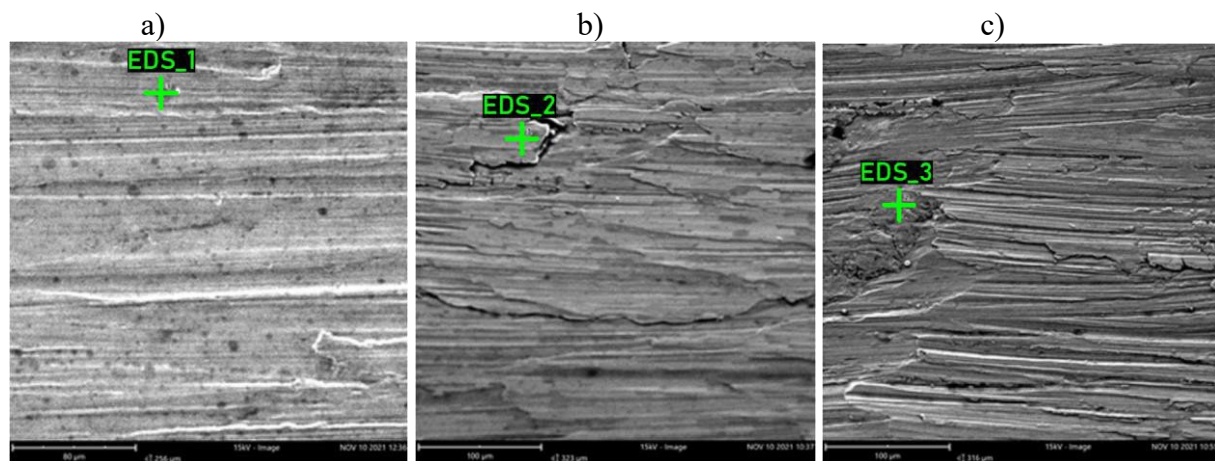


Fig. 9. SEM images of the inner surface of the drawpieces with marked points of chemical composition analysis using the EDS method, for variants, respectively: Base parameters (a), high feed rate (b), and high rotational speed (c).

Table 2. Chemical composition (at%) of the EDS points.

Point analyzed	Percentage weight concentration (%)		
	Zn	Fe	C
EDS 1	100	-	-
EDS 2	78.94	7.20	13.86
EDS 3	13.44	48.00	38.56

Conclusion

This paper presents the results of preliminary experimental studies aimed at determining the possibility of forming stiffening ribs in Litecor sandwich composites. Plastic shaping using the SPIF method was considered, and effective parameters were indicated to ensure the production of embossing of the correct quality in terms of surface characteristics and cross-section. The most important conclusions of the described research work are listed below.

1. Litecor layered composites composed of steel covers can be successfully shaped using the SPIF method, and the maximum depth for the stiffening ribbing geometry presented in the paper is $D = 5.65$ mm. Above this value, the orange peel phenomenon appears in the embossing most stressed area of the outer surface of the embossing, and with a further increase in the tool recess, cracking of the outer cover occurs. Cracking is always initiated at the end of an embossing.

2. Significant thinning of the material was demonstrated in the cross-embossed section, namely 56.2%. The greatest reduction in thickness was found in the corner of the rib. As for the change in the thickness of individual layers in this cross-section, the thickness of the polymer core was reduced here by 62.9%. In turn, the covers were reduced by 50% and by 46.7% for the inner and outer cover respectively. In the case of the polymer core, the degree of deformation indicates only an elastic deformation, while the steel covers underwent plastic deformation, and the degree of this deformation indicates a significant strengthening of the material in this area.

3. The paper shows that the adopted basic kinematic parameters of forming stiffening ribs, i.e. tool rotational speed $n = 300$ rpm, feed rate $f = 1500$ mm/min, enable the embossing surface to be obtained without damaging the zinc layer, thus without damaging the anti-corrosion coating. On the other hand, a tenfold increase in rotational speed to $n = 3000$ rpm, due to the friction phenomena that occur, leads to the scuffing of the zinc coating, which is evidenced by the predominant presence of iron on the shaped surface. Doubling the feed rate also breaks the zinc coating.

References

- [1] T. Cao, B. Lu, D. Xu, H. Zhang, J. Chen, H. Long, J. Cao, An efficient method for thickness prediction in multi-pass incremental sheet forming. *Int. J. Adv. Manuf. Technol.* 77 (2015) 469–483.
- [2] G. Ingarao, R. Di Lorenzo, F. Micari, Sustainability issues in sheet metal forming processes: An overview. *J. Clean. Prod.* 19 (2011) 337–347.
- [3] Q. Zhang, F. Xiao, H. Guo, C. Li, L. Gao, X. Guo, W. Han, A. Bondarev, Warm negative incremental forming of magnesium alloy AZ31 Sheet: New lubricating method. *J. Mater. Process. Technol.* 210 (2010) 323–329.
- [4] G. Ambrogio, L. Filice, F. Gagliardi, Formability of lightweight alloys by hot incremental sheet forming. *Mater. Des.* 34 (2012) 501–508.
- [5] W. Bao, X. Chu, S. Lin, J. Gao, Experimental investigation on formability and microstructure of AZ31B alloy in electropulse-assisted incremental forming. *Mater. Des.* 87 (2015) 632–639.
- [6] G. Ambrogio, L. De Napoli, L. Filice, F. Gagliardi, M. Muzzupappa, Application of incremental forming process for high customised medical product manufacturing. *J. Mater. Process. Technol.* 162 (2005) 156–162.
- [7] L. Galdos, E.S. De Argandoña, I. Ulacia, G. Arruebarrena, Warm incremental forming of magnesium alloys using hot fluid as heating media. *Key Engineering Materials*, vol. 504-506 (2012) 815-820.
- [8] L. Fratini, G. Ambrogio, R. Di Lorenzo, L. Filice, F. Micari, Influence of mechanical properties of the sheet material on formability in single point incremental forming, *CIRP Annals-Manufacturing Technology* 53(1) (2004) 207-210.
- [9] L. Filice, L. Fratini, F. Micari, Analysis of material formability in incremental forming, *CIRP annals-Manufacturing technology* 51(1) (2002) 199-202.
- [10] T.A. Marques, M.B. Silva, P.A.F. Martins, On the potential of single point incremental forming of sheet polymer parts, *The International Journal of Advanced Manufacturing Technology* 60(1-4) (2012) 75-86.
- [11] I. Bagudanch, M.L. Garcia-Romeu, M. Sabater, Incremental forming of polymers: process parameters selection from the perspective of electric energy consumption and cost, *Journal of Cleaner Production* 112 (2016) 1013-1024.
- [12] G. Centeno, M.B. Silva, V.A.M. Cristino, C. Vallellano, P.A.F. Martins, Hole-flanging by incremental sheet forming. *International Journal of Machine Tools and Manufacture* 59 (2012) 46- 54.

-
- [13] R. Conte, G. Ambrogio, D. Pulice, F. Gagliardi, L. Filice, Incremental Sheet forming of a composite made of thermoplastic matrix and glass-fiber reinforcement. *Procedia Engineering* 207 (2017) 819–824.
- [14] J. Jeswiet, J.R. Duflou, A. Szekeres, Forces in single point and two point incremental forming. *Adv. Mater. Res.* 6–8 (2005) 449–456.
- [15] J.R. Duflou, A. Szekeres, P. Vanherck, Force measurements for single point incremental forming: An experimental study. *Adv. Mater. Res.* 6–8 (2005) 441–448.
- [16] J. Duflou, B. Callebaut, J. Verbert, H. De Baerdemaeker, Laser assisted incremental forming: Formability and accuracy improvement. *CIRP Ann. Manuf. Technol.* 56 (2007) 273–276.
- [17] J. Duflou, B. Callebaut, J. Verbert, H. De Baerdemaeker, Improved SPIF performance through dynamic local heating. *Int. J. Mach. Tools Manuf.* 48 (2008) 543–549.
- [18] L. Filice, G. Ambrogio, F. Micari, On-line control of single point incremental forming operations through punch force monitoring. *CIRP Ann. Manuf. Technol.* 55 (2006) 245–248.
- [19] G. Centeno, I. Bagudanch, A. Martínez-Donaire, M.L. Garcia-Romeu, C. Vallsellano, Critical analysis of necking and fracture limit strains and forming forces in single-point incremental forming. *Mater. Des.* 63 (2014) 20–29.
- [20] D. Xu, W. Wu, R. Malhotra, J. Chen, B. Lu, J. Cao, Mechanism investigation for the influence of tool rotation and laser surface texturing (LST) on formability in single point incremental forming. *Int. J. Mach. Tools Manuf.* 73 (2013) 37–46.
- [21] G. Palumbo, M. Brandizzi, Experimental investigations on the single point incremental forming of a titanium alloy component combining static heating with high tool rotation speed. *Mater. Des.* 40 (2012) 43–51.
- [22] G. Hussain, L. Gao, N. Hayat, Z. Cui, Y. Pang, N. Dar, Tool and lubrication for negative incremental forming of a commercially pure titanium sheet. *J. Mater. Process. Technol.* 203 (2008) 193–201.
- [23] N.G. Azevedo, J.S. Farias, R.P. Bastos, P. Teixeira, J.P. Davim, R.J.A. de Sousa, Lubrication aspects during single point incremental forming for steel and aluminum materials. *Int. J. Precis. Eng. Manuf.* 16 (2015) 589–595.
- [24] I. Bagudanch, G. Centeno, C. Vallsellano, M. Garcia-Romeu, Forming force in single point incremental forming under different bending conditions. *Procedia Eng.* 63 (2013) 354–360.
- [25] A.D. Brooker, J. Ward, L. Wang, Lightweighting impacts on fuel economy, cost, and component losses. *SAE Technical Papers* 2 (2013).
- [26] E. Alonso, T. Lee, C. Bjelkengren, R. Roth, R. Kirchain, Evaluating the Potential for Secondary Mass Savings in Vehicle Lightweighting. *Environmental Science & Technology*, 46(5) (2012) 2893– 2901.
- [27] S. To et al., *Cars on a Diet : 1 The Material and Energy Impacts of Passenger Vehicle Weight Reduction in the U.S.* (2010).
- [28] J.S. Tanco, C.V. Nielsen, A. Chergui, W. Zhang, N. Bay, Weld nugget formation in resistance spot welding of new lightweight sandwich material. *Int. J. Adv. Manuf. Technol.* 80 (2015) 1137– 1147.
- [29] S. Amancio-Filho, J. Dos Santos, Joining of polymers and polymer-metal hybrid structures: Recent developments and trends. *Polym. Eng. Sci.* 49 (2009) 1461–1476.
- [30] T.R.M. Contreiras, J.P.M. Pragana, I.M.F. Bragança, C.M.A. Silva, L.M. Alves, P.A.F. Martins, Joining by forming of lightweight sandwich composite panels. *Procedia Manuf.* 29 (2019) 288–295.

-
- [31] T.R.M. Contreiras, Joining by Forming of Composite Sandwich Panels. Master's Thesis, Mechanical Engineering, Técnico Lisboa, Portugal, February (2019).
 - [32] Springer Fachmedien Wiesbaden. Application Potential of Litecor in the Body. In ATZextra Worldwide; Springer Fachmedien Wiesbaden: Wiesbaden, Germany (2014) 108–111.
 - [33] R. Haque, Quality of self-piercing riveting (SPR) joints from cross-sectional perspective: A review. *Arch. Civ. Mech. Eng.* 18 (2018) 83–93.
 - [34] ThyssenKrupp Steel Europe AG. Technische Daten für Litecor C, 04 (2015).
 - [35] J. Slota, A. Kubit, T. Trzepieciński, B. Krasowski, J. Varga, Ultimate Load-Carrying Ability of Rib-Stiffened 2024-T3 and 7075-T6 Aluminium Alloy Panels under Axial Compression. *Materials* 14, 1176, (2021) 1-19.
 - [36] B. Krasowski, A. Kubit, T. Trzepieciński, J. Slota, Experimental analysis of single point incremental forming of truncated cones in DC04 steel sheet. *Advances in Materials Science*, Vol. 20, No. 4(66), December (2020) 5-15.
 - [37] M. Durante, A. Formisano, A. Langella, F.M.C. Minutolo, The influence of tool rotation on an incremental forming process. *J. Mater. Process. Technol.* 209 (2009) 4621–4626.
 - [38] D. Xu, W. Wu, R. Malhotra, J. Chen, B. Lu, J. Cao, Mechanism investigation for the influence of tool rotation and laser surface texturing (LST) on formability in single point incremental forming. *Int. J. Mach. Tools Manuf.* 73 (2013) 37–46.